

Probing solar accelerated particles with Konus-Wind data

Alexandra Lysenko¹,
Sergey Anfinogentov², Dmitry Svinkin¹, Dmitry Frederiks¹,
Gregory Fleishman^{3,1}, Alexander Altyntsev², Nataliia Meshalkina²,
Larisa Kashapova², Hugh Hudson^{4,5},
and the *Konus-Wind* team

¹ Ioffe Institute, Saint-Petersburg, Russian Federation

² Institute of Solar-Terrestrial Physics, Irkutsk, Russian Federation

³ New Jersey Institute of Technology, Newark, USA

⁴ School of Physics and Astronomy, University of Glasgow, Glasgow, UK

⁵ UC Berkeley, Berkeley, USA

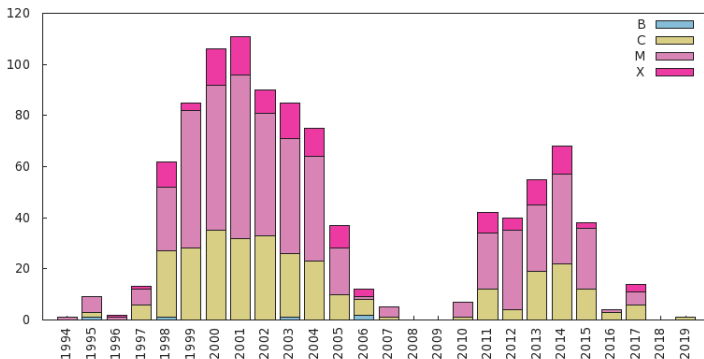
2019



**Ioffe Workshop on GRBs
and other Transient Sources:
25 years of Konus-Wind**

September 9–13, 2019, St.Petersburg, Russia

- Summary of *Konus-Wind* solar observations.
- Advantages of *Konus-Wind* for solar flare physics.
- Short elementary bursts as the probe for electron acceleration.
- Gamma-ray emission and ion acceleration.
- The puzzle of behind-the-limb flares.



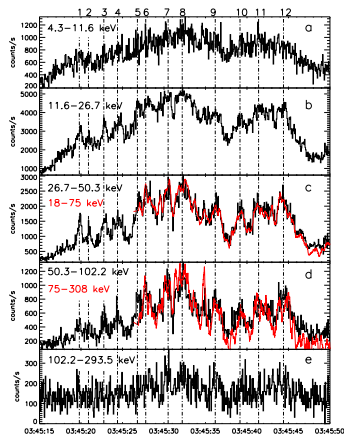
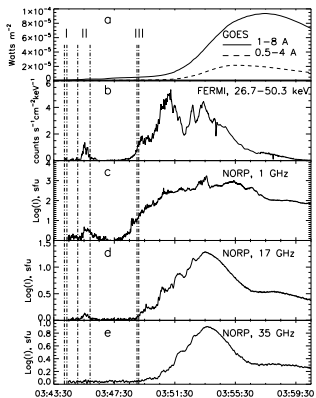
Since 1994 Konus-Wind observed

- ~13000 solar flares in the waiting mode,
- 1042 solar flares in the triggered mode and among them,
- 94 solar flares at energies > 1 MeV.
- All the data on solar flares registered by Konus-Wind in the triggered mode are available online via <http://www.ioffe.ru/LEA/kwsun>.

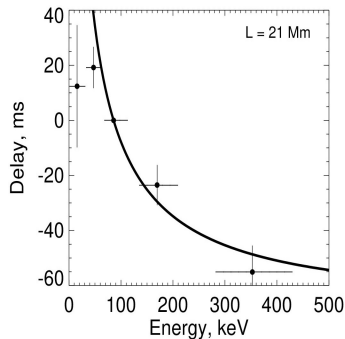
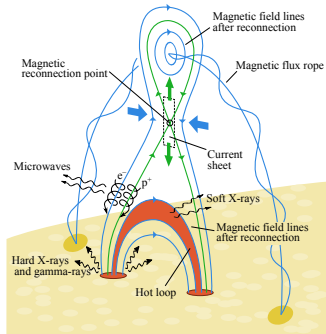
- Operates since November 1, 1994 till present time – more than two full solar cycles.
- Continuous observations of the Sun in the 20–1200 keV band in the waiting mode. *Konus-Wind* is an analogue of GOES instrument in Hard X-rays.
- High time resolution (up to 2 ms) in the triggered mode.
- Energy range in the triggered mode (~ 20 keV–15 MeV) covers emission from accelerated particles (both electrons and ions).

Elementary bursts and electron acceleration

- What are the shortest acceleration time scales?
- Are short bursts and longer bursts produced by different acceleration mechanisms?
- Are longer bursts superposition of shorter bursts?
- We selected short “elementary” bursts for estimation of electric field accelerating the particles.



Elementary bursts and electron acceleration

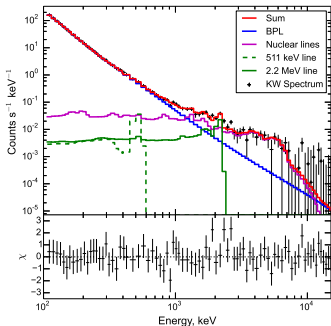


- Acceleration times $t_{acc} < 50$ ms.
- Electron energy $E \sim 500$ keV.
- Acceleration length $L_{acc} \sim \langle v \rangle t_{acc} \sim 10$ Mm.
- Electric field $E > A/L_{acc} \sim 0.1$ V/m, which is one order of magnitude larger than the typical values of the Dreicer field ($\sim 10^{-2}$ V/m).

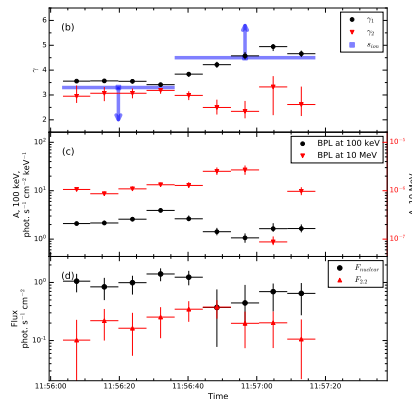
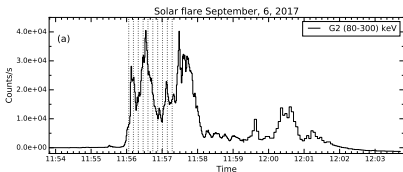
“Rapid Variability in the SOL2011-08-04 Flare: Implications for Electron Acceleration” Altyntsev et al., 2019, ApJ, in press

- The strongest solar flare of solar cycle # 24 in soft X-rays.
- One of the strongest photospheric magnetic field $\sim 5,500$ G (Wang et al. 2018) and strongest coronal magnetic field $\sim 4,000$ G (Anfinogentov et al. 2019) ever observed.
- Impulsive phase occurred during “nights” of both *RHESSI* and *Fermi*.

“Gamma-ray emission from the impulsive phase of the 2017 September 6 X9.3 flare” Lysenko et al., 2019, *ApJ*



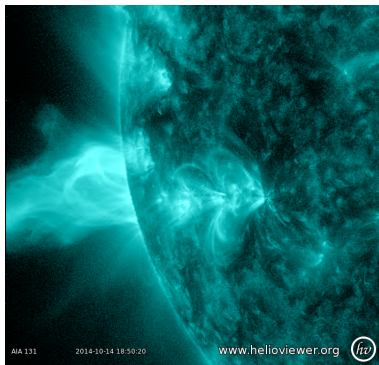
- Accelerated electrons and positrons produced in nuclear reactions
→ continuum, BPL model.
- Accelerated ions → nuclear reactions
→ nuclear deexcitation lines (~ 2 – 30 MeV ions),
→ neutrons → neutron capture line at 2.2 MeV (~ 20 – 300 MeV ions),
→ positrons → positron-electron annihilation line at 511 keV (from ~ 2 MeV to >300 MeV).



- Low energy part of continuum shows soft-hard-soft evolution.
- **BPL power law indices and amplitudes at 100 keV and 10 MeV do not correlate!**
 - Second stage electron acceleration?
 - Contribution from the ultrarelativistic positrons?
 - Other than bremsstrahlung emission mechanisms?
- Ratio of neutron production rate to nuclear deexcitation lines fluxes $F_{nuclear}$ is very sensitive to the power law index s_{ion} of the accelerated ions.
- Based on time evolution of $F_{2.2}$ and $F_{nuclear}$ we estimated limits for s_{ion} with high (~ 30 s) time resolution.
- **Power law index of the low energy part of the continuum and ion power law index do correlate!**

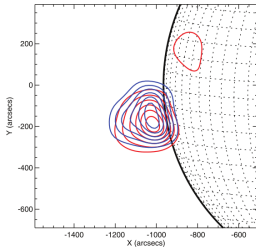
“Ordinary flare”

- Correlation between time profile in hard X-rays and derivative of time profile in soft X-rays – Neupert effect.
- Soft-hard-soft spectral evolution in hard X-rays.

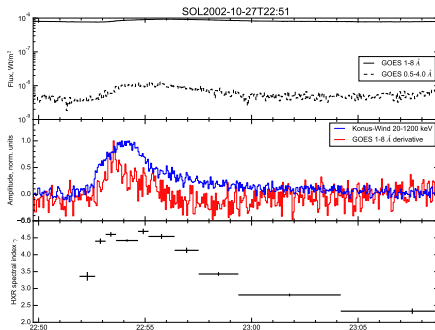


- BTL flare footpoints are located rather far (10–50 degrees) behind the solar limb.
- We observe high coronal sources, stronger footpoint emission is occulted by the limb.
- BTL often show very different behavior relative to “ordinary” flares.

Krucker, White, Lin, 2007, *Astrophys. journal*.

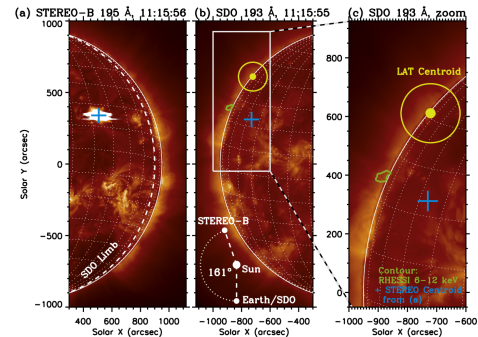
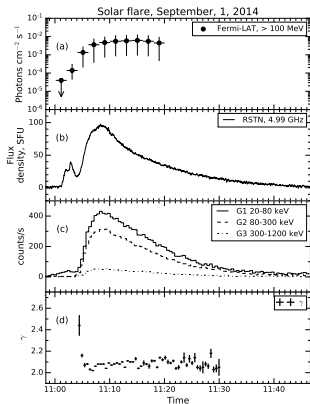


- Was located $\sim 50^\circ$ behind the solar limb.
- Demonstrated hard-soft-hard spectral evolution.
- Low response in soft X-rays (GOES 1–8 Å band).
- Soft X-rays derivative is ahead of hard X-rays.



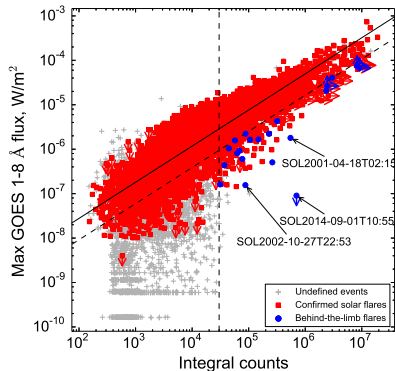
Ackermann et al., 2017, Astrophys. journal.

- Was located $\sim 44^\circ$ behind the solar limb.
- Stereoscopic observations were performed by *STEREO-B* spacecraft.
- No response in soft X-rays (GOES 1–8 Å band).
- High correlation between hard X-rays, microwaves and gamma-rays > 100 MeV.
- No spectral evolution in hard X-rays, spectral index $\gamma \sim 2$.



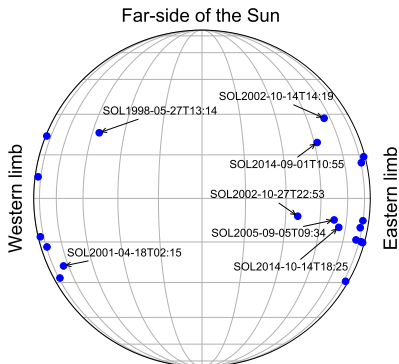
Search for behind-the-limb flares in homogeneous *Konus-Wind* waiting mode observations

- Criterium for behind-the-limb candidate selection was low response in GOES 1–8 Å channel relative to intensity in *Konus-Wind*.
- This criterium yielded ~ 300 behind-the-limb candidates out of ~ 16000 events.
- For these candidates we used localisations from different instruments (*RHESSI*, *NoRP*, *OVSA Nancy*).



Search for behind-the-limb flares in homogeneous *Konus-Wind* waiting mode observations

- We found 20 behind-the-limb flares including 3 known from previous studies.



“Catalog of behind-the-limb solar flares registered by the *Konus-Wind* instrument in 1994–2019 yy.” Lysenko et al., in preparation

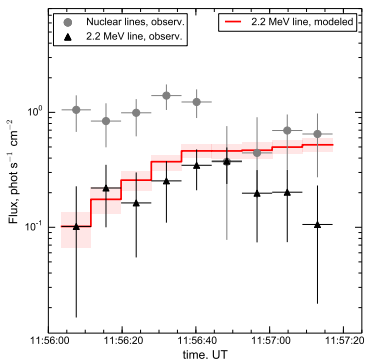
- “Sources of Quasi-periodic Pulses in the Flare of 18 August 2012” by Altyntsev et al., 2016, SolPhys.
- “A Cold Flare with Delayed Heating” by Fleishman et al., 2016, ApJ.
- “Fermi-LAT Observations of High-energy Behind-the-limb Solar Flares” by Ackermann et al., 2017, ApJ.
- “Flare SOL2012-07-06: On the Origin of the Circular Polarization Reversal Between 17 GHz and 34 GHz” by Altyntsev et al., 2017, SolPhys.
- “Statistics of “Cold” Early Impulsive Solar Flares in X-Ray and Microwave Domains” by Lysenko et al., 2018, ApJ.
- “Onset of Photospheric Impacts and Helioseismic Waves in X9.3 Solar Flare of 2017 September 6” by Sharykin & Kosovichev, 2018, ApJ.
- “Radio, Hard X-Ray, and Gamma-Ray Emissions Associated with a Far-Side Solar Event” by Grechnev et al., 2018, SolPhys.
- “Electron Acceleration and Jet-facilitated Escape in an M-class Solar Flare on 2002 August 19” by Glesener & Fleishman, 2018, ApJ.
- “Characteristics of Late-phase >100 MeV Gamma-Ray Emission in Solar Eruptive Events” by Share et al., 2018, ApJ.
- “Gamma-Ray Emission from the Impulsive Phase of the 2017 September 6 X9.3 Flare” by Lysenko et al., 2019, ApJ.

Thank you for attention

Temporal evolution of the 2.223 MeV line **in the absence of the ion spectral evolution** can be described as (Prince et al., 1983):

$$F_{2.2}(t) \propto \int_{-\infty}^t S(t') R(t, t') dt' \quad (1)$$

where $S(t')$ – is the neutron production time profile $\propto F_{nuclear}$, $R(t, t')$ – response function, giving 2.223 MeV line at time t from a neutron born at time $t' \propto \exp(-(t - t')/\tau)$, $\tau \sim 100$ s Murphy et al., 2007.

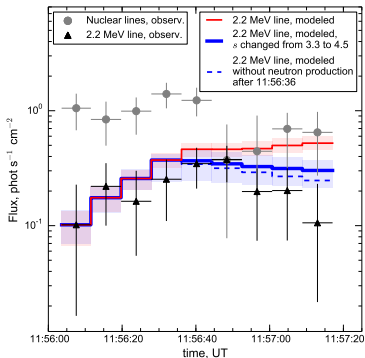


We replace the integral by the sum (Kurt et al., 2017):

$$F_{2.2}(t_i) \propto \sum_{j=0}^i F_{4-7}(t_j) \exp\left(-\frac{t_i - t_j}{\tau}\right) \Delta t_j \quad (2)$$

The reason of the discrepancy between data and modeling is the decrease of neutron production after 11:56:36. **Why?**

- Neutron production reduced at least in $r_n \sim 5$ times.
- Possible reason – abrupt steepening of the ion spectrum after the main peak.



Taking the mean ion power index $s_{mean} \sim 4$ and the neutron reduction rate $r_n \sim 5$ we estimated upper limit for s_{before} before the peak and the lower limit for s_{after} after the main peak.

